

# Progressive Spatial Recurrent Neural Network for Intra Prediction

Yueyu Hu, *Student Member, IEEE*, Wenhan Yang, *Student Member, IEEE*, Mading Li,  
and Jiaying Liu, *Senior Member, IEEE*

**Abstract**—Intra prediction is an important component of modern video codecs, which is able to efficiently squeeze out the spatial redundancy in video frames. With preceding pixels as the context, traditional intra prediction schemes generate linear predictions based on several predefined directions (*i.e.* modes) for blocks to be encoded. However, these modes are relatively simple and their predictions may fail when facing blocks with complex textures, which leads to additional bits encoding the residue. In this paper, we design a Progressive Spatial Recurrent Neural Network (PS-RNN) that learns to conduct intra prediction. Specifically, our PS-RNN consists of three spatial recurrent units and progressively generates predictions by passing information along from preceding contents to blocks to be encoded. To make our network generate predictions considering both distortion and bit-rate, we propose to use Sum of Absolute Transformed Difference (SATD) as the loss function to train PS-RNN since SATD is able to measure rate-distortion cost of encoding a residue block. Moreover, our method supports variable-block-size for intra prediction, which is more practical in real coding conditions. The proposed intra prediction scheme achieves on average 2.4% bit-rate reduction on variable-block-size settings under the same reconstruction quality compared with HEVC.

**Index Terms**—Video Coding, Intra Prediction, Deep Learning, Spatial RNN, SATD Loss, HEVC

## I. INTRODUCTION

**I**NTRA prediction efficiently reduces spatial redundancy in videos and improves video coding performance. It has been adopted in modern codecs like H.264/AVC [1] and HEVC [2]. Compared with H.264/AVC, HEVC achieves a leap in rate-distortion performance by enriching reference samples and enlarging the number of angular modes in intra prediction. Besides, HEVC adopts a more flexible quadtree coding structure, which adaptively chooses the appropriate block size during the coding process. However, there are some drawbacks in traditional intra prediction schemes. On one hand, modern codecs only use a single line of preceding reconstructed pixels above and on the left side of the current prediction unit (PU) as the reference to generate predictions, which can be affected by the noise (*e.g.* quantization noise) in the reconstructed pixels. On the other hand, for directional intra prediction in HEVC, only Planar, DC and other 33 angular modes are utilized. None of above can handle complex texture even with Rate-Distortion Optimization (RDO) [3].

To address the drawbacks of the single-line reference scheme, improved intra prediction with multi-line reference scheme [4, 5] or using filtered reference samples [6] are investigated. Furthermore, to enhance the ability of HEVC intra prediction for complex textures, synthesis-based methods [7], copying-based methods [8, 9] and inpainting-based

methods [10, 11] are developed. Although these methods mitigate the problems, each of them has limitations. Though some methods adopt the multi-line reference scheme, the contextual information of reference pixels is usually not utilized. Besides, the performance of copying-based methods is limited by the structural similarities of intra patches, while inpainting-based methods are not capable of accurately predicting the pixels at the bottom-right of the current PU.

In the past decade, Deep Neural Network (DNN), as an effective data-driven solution for computer vision tasks, has been exploited to accomplish visual recognition, image generation and image enhancement tasks. With powerful computing devices like GPUs and TPUs [12], given well-defined inputs and outputs, the network can automatically learn the end-to-end mapping from inputs to outputs. This technique has been utilized in video coding tasks like fractional interpolation [13], deblocking [14] and fast mode decision [15]. It can also facilitate intra prediction. Pioneering works that utilize deep learning models in intra prediction explores the potential of Fully-Connected (FC) neural networks [16] and Convolutional Neural Networks (CNN) [17]. As they are all end-to-end approaches, the issues of quantization noise and the inability of handling complex texture are addressed jointly.

However, several important issues are neglected in these previous works:

- For FC networks, they take vectors as inputs, which neglect the spatial correlations in reference blocks. As for CNN-based methods, they are not suited for the task of intra prediction problem, in which the reference inputs are asymmetric (*i.e.*, reference pixels are above and on the left side of the current PU). Convolutions at the bottom-right of the current PU cannot propagate any information.
- Commonly used Mean Squared Error (MSE) loss measures the pixel-wise distortion of the prediction. However, a lower MSE between the the prediction signals and the original block does not indicate better rate-distortion performance in video coding. Thus, MSE is not a promising guidance and constraint to train networks for intra prediction.
- Methods mentioned above are only implemented in fixed-block-size configuration. However, practical codecs often use variable block sizes to deal with contents with difference scales. Only supporting a fixed block size severely limits the coding performance, making these methods less practical in real coding conditions.

In this paper, we aim to address the drawbacks of traditional

intra prediction schemes and aforementioned deep learning based methods. Specifically, we build an end-to-end trainable Progressive Spatial Recurrent Neural Network (PS-RNN) to learn to predict contents of PUs in intra prediction. Three spatial recurrent units are stacked sequentially, which update and aggregate internal memory progressively along certain directions (*i.e.* horizontal and vertical in our work), facilitating the modeling capacity of PS-RNN. To further improve the coding performance of our method, we propose to use SATD as the training loss of PS-RNN. SATD not only calculates the distortion but also reflects bit-rate, thus it is a good criterion to guide the network training for intra prediction. Moreover, our method enables variable-block-size configuration, which further reduces bit-rate and makes the method practical for video coding applications. Unlike traditional intra prediction schemes, we use preceding blocks instead of preceding single lines as reference input to generate predictions.

To summarize, our contributions are listed as follows:

- We propose an end-to-end trainable neural network for intra prediction. The network takes block references as its input. Experimental results demonstrate that this deep learning method achieves superior performance compared with methods using single lines as reference, especially when facing of severe quantization noises in low-bit-rate configurations and complex textures.
- A progressive spatial RNN is specially designed for intra prediction. It infers information from reference inputs to the current PU progressively along certain directions resulting in consistent and accurate predictions.
- In order to make our network generate predictions with less distortion and lower bit-rate, we propose to use SATD as training loss function. Compared to MSE, using SATD as loss function largely improves the rate-distortion performance of the codec.
- Our model supports variable-block-size configuration, which makes our method practical for video coding applications. Allowing variable-block-size coding significantly reduces bit-rate especially for high-resolution videos.

The rest of the paper is organized as follows. In Section II, we review related works on deep learning for intra prediction for video coding and deep learning for image compression. Section III introduces our proposed intra prediction. We formulate the problem and analyze the proposed PS-RNN trained with SATD loss function in detail. In Section IV, we show our gain in rate-distortion performance compared with HEVC and previous methods. We visually and quantitatively compare the predictions of our method and other methods to explain where the improvement comes from. Finally in Section V, we draw a conclusion of this paper.

## II. RELATED WORK

### A. Intra Prediction for Video Coding

Modern codecs usually consist of multiple parts to progressively squeeze out redundancy and reduce the bit-rate [18, 1]. In this work, we focus on the intra prediction component of video coding methods. In HEVC, 35 intra prediction modes are assembled with RDO to predict for the encoding block,

including Planar mode and DC mode. DC mode fills the block with DC signals. If Planar mode is selected, each pixel of the block is generated by a linear combination of corresponding pixels in the reference samples. For the other 33 modes, the prediction signals are generated according to reconstructed pixels on predefined directions. However, this reference scheme sometimes fails in some tough cases, especially for low-bit-rate coding conditions and frames with complex textures. To overcome this vulnerability to noise, intra prediction involving multiple reference lines is developed to jointly taking additional reference lines as reference samples [4, 5]. It significantly reduces the impact of the noise.

Involving deep models in intra coding for videos has been initially studied in recent years. Deep neural networks can automatically learn the end-to-end mapping of inputs and outputs. It can also be easily accelerated using large-scale parallel programming. In [15], CNN has been utilized for mode decision as it has a strong potential of capturing global feature from image data. In [16, 17] fully-connected (FC) network and CNN are exploited directly in intra prediction. By training a network to build a mapping from the reference samples to the prediction signal, FC networks and CNN show improvement in rate-distortion performance compared with HEVC.

There are two main problems for the deep-network-based intra prediction methods. On one hand, the network is usually trained using pixel-wise MSE loss function. But the final coding cost is also influenced by the correlations between adjacent pixels. Thus, two predictions with similar MSE can have a much different coding cost. On the other hand, CNN is not capable of handling asymmetric image completion tasks, as the whole input block is convolved unconditionally. Large areas with no texture information interferes the extraction of spatial features. To address these issues, we proposed the spatial RNN for intra prediction with SATD loss function. The network progressively handles prediction contexts, mitigating the influence of asymmetric distribution of reference pixels. Besides, SATD is utilized as the loss function for training. In HEVC, SATD is widely used to measure the rate-distortion cost of encoding a residue block. Since it applies a time-frequency transformation to the difference, it can jointly measure the pixel-wise difference and the contextual difference. As a result, SATD is more consistent with the real coding cost than MSE.

### B. Deep Learning for Image Compression

Compression of videos and images shares the same philosophy as videos can be seen as stacks of images. HEVC also supports encoding images in the still image profile [19]. Image codecs are relatively simpler than video codecs. So deep learning is first explored for image compression and then extended to videos. There have been several approaches to utilize deep neural networks for lossy image compression. These approaches are mostly based on autoencoders [20, 21, 22, 23] and convolutional recurrent neural networks [24, 25]. These methods achieve impressive visual quality with low coding bit-rate and the performance is superior to conventional image

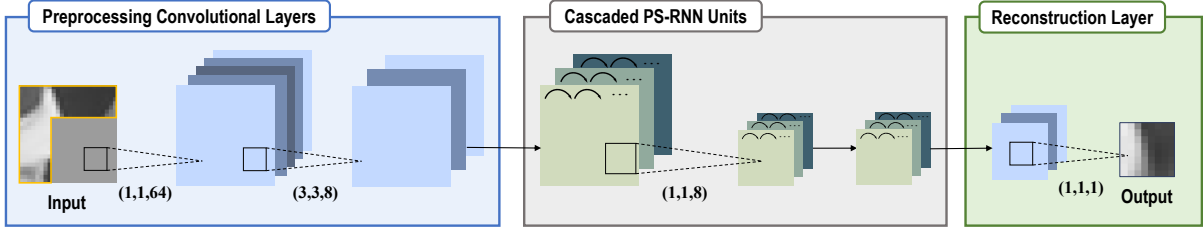


Fig. 1: Architecture of PS-RNN. Preprocessing convolutional layers map the input image into feature space. After the preprocessing, the feature maps are handled by cascaded PS-RNN units. A spatial down-sampling is performed on the output of the first PS-RNN unit, making the feature maps identical to the PU in spatial scale. A convolutional reconstruction layer maps the predicted feature maps to pixel space.

codecs like JPEG and JPEG2000. However, these approaches still face challenges for high bit-rate conditions. Besides, even in low bit-rate conditions, they are not yet comparable with intra coding in HEVC still image profile. These methods for image compression are still far from being adopted in video codecs. Different from the methods mentioned above, in our work, we focus on optimizing the intra prediction scheme in the loop of video coding.

### C. Image Inpainting for Intra Prediction

Intra prediction shares similar characteristics with image inpainting, which aims to accurately fill in the missing areas of an image. Previous works on image inpainting study the methods to propagate information from neighboring known pixels to missing areas or to copy similar patches to unknown regions [26, 27, 28, 29]. Recently, works studying learning based image inpainting emerge. These methods typically utilize CNN to directly maps input images with unknown regions to restored output image [30, 31].

Image inpainting techniques have been employed in image and video coding [11, 25, 10]. However, unlike the original inpainting task where the unknown regions are relatively small and usually surrounded by known pixels, in intra prediction, only the preceding pixels are available. Predicting the pixels on the right below of the current PU is hard as this area is too far from the reference. Inpainting based methods face challenges in intra prediction.

Different from previous works on image inpainting methods, we take the unique structure of intra prediction context into consideration. The predictions are generated in a progressive way. Thus, the prediction for the hard regions can take previously filled regions as the reference.

## III. PS-RNN FOR INTRA PREDICTION

In this section, we present a detailed description and analysis of the proposed PS-RNN. We first formulate the problem, where we conduct the prediction in feature space. Then we illustrate the overall framework of the network. After that we investigate the SATD loss function for training a network for intra prediction. At last, we show how the proposed network is integrated with HEVC with variable-block-size configuration.

### A. Formulation of Progressive Prediction

Our goal is to accurately fill in the missing block given the existing pixels on the left and above. To achieve the goal, we formulate intra prediction as a progressive prediction problem. The prediction is conducted on feature space. Given an image representing the input context, we first transform the image to feature space using convolutions. We define the resulting feature maps which have  $c$  channels  $n$  rows and  $n$  columns as  $\mathbf{X}_{n,n,c}$ . It is viewed as a stack of horizontal planes  $\mathbf{X}^h = \{\mathbf{X}_{0,\cdot,\cdot}, \mathbf{X}_{1,\cdot,\cdot}, \dots, \mathbf{X}_{n-1,\cdot,\cdot}\}$  or a stack of vertical planes  $\mathbf{X}^v = \{\mathbf{X}_{\cdot,0,\cdot}, \mathbf{X}_{\cdot,1,\cdot}, \dots, \mathbf{X}_{\cdot,n-1,\cdot}\}$ , where each element in the stack represents a feature vector. Note that both stacks represent the original block  $\mathbf{X}_{n,n,c}$  but are sliced in vertical and horizontal, respectively. Our goal is to generate the predictions of the feature vectors given previous observations in the sequence. We take the horizontal split as an example. Under the assumption that the distribution of local features is continuous, this process can be formulated as,

$$\tilde{\mathbf{X}}_i^h = \mathcal{F}(\mathbf{X}_i^h, \mathbf{X}_{i-1}^h, \theta), \quad (1)$$

where  $\tilde{\mathbf{X}}_i^h$  is the predicted feature vector for the  $i^{th}$  line and  $\mathcal{F}()$  is the function to generate the prediction signals from previous observations together with the current input feature vector. Note that during prediction,  $\mathbf{X}_i^h$  only contains partial reference information, so the function  $\mathcal{F}()$  learns to adjust its attention and leans on the informative observation  $\mathbf{X}_{i-1}^h$ . After the progressive prediction, the vertical and horizontal prediction signals are then fused to form the output feature maps. Further more, to make the intra-prediction more precise, we conduct the progressive prediction several times.

### B. Overall Framework

Based on Eq. (1), we design PS-RNN for improved intra prediction in HEVC. The architecture of the network is shown in Fig. 1. In the preprocessing CNN, convolutional layers extract local features of the input context block and transforms the image to feature space. This process also removes noise in the reference pixels by learned filters. After the transformation, a PS-RNN unit is connected to the output of the convolutional layer to provide initial prediction. The structure of PS-RNN unit is described in detail in Fig. 2. As deeper networks provide

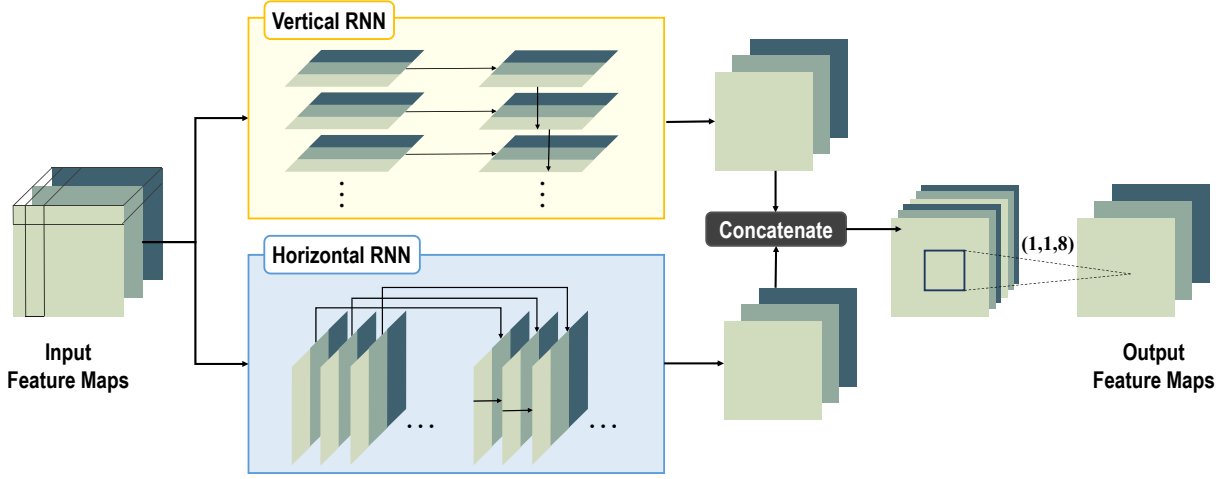


Fig. 2: Structure of a PS-RNN unit. It splits a stack of feature maps into vertical and horizontal planes. Each plane represents a feature map of a vertical line or a horizontal line in the original grey-scale image. After the progressive prediction, these planes are concatenated to reconstruct the feature maps. A convolutional layer is used to fuse the predictions from the vertical and horizontal feature maps.

improved learning ability, more PS-RNN units are cascaded to repeat the prediction process. While making the network deeper, we control the complexity by down-sampling the feature maps. At the end of the progressive generation, the outputs of the last PS-RNN unit are transformed back to pixel space with the reconstruction layer.

The structure of the PS-RNN unit is shown in Fig. 2. In each unit, the input feature tensor is split to horizontal and vertical lines, respectively. Suppose the shape of the feature tensor is  $(n, n, c)$ , with  $c$  to be the number of channels. It is split to  $\mathbf{X}^h = \{\mathbf{X}_{0,\cdot,\cdot}, \mathbf{X}_{1,\cdot,\cdot}, \dots, \mathbf{X}_{n-1,\cdot,\cdot}\}$  and  $\mathbf{X}^v = \{\mathbf{X}_{\cdot,0,\cdot}, \mathbf{X}_{\cdot,1,\cdot}, \dots, \mathbf{X}_{\cdot,n-1,\cdot}\}$ . Each element in  $\mathbf{X}^h$  or  $\mathbf{X}^v$  is a feature map of shape  $(n, c)$ . We take the horizontal form as an example. To conduct recurrent learning, each element of shape  $(n, c)$  in the sequence is flattened to a vector of  $n \times c$  dimensions. We define the  $t$ -th feature vector in the sequence as  $\mathbf{x}_t$ . The definition of  $\mathbf{X}^h$  can be simplified as  $\mathbf{X}^h = \{\mathbf{x}_0, \mathbf{x}_1, \dots, \mathbf{x}_{n-1}\}$ . For each stack of feature vectors, an RNN with Gated Recurrent Units (GRU) is used to progressively generates prediction signals. This process is formulated as follows,

$$\begin{aligned}
 \mathbf{z}_t &= \sigma(\mathbf{W}^z \mathbf{x}_t + \mathbf{U}^z \mathbf{h}_{t-1}), \\
 \mathbf{r}_t &= \sigma(\mathbf{W}^r \mathbf{x}_t + \mathbf{U}^r \mathbf{h}_{t-1}), \\
 \mathbf{h}_t &= \mathbf{z}_t \odot \mathbf{h}_{t-1} + (1 - \mathbf{z}_t) \odot \\
 &\quad \sigma(\mathbf{W} \mathbf{x}_t + \mathbf{U}(\mathbf{r}_t \odot \mathbf{h}_{t-1}) + \mathbf{b}),
 \end{aligned} \tag{2}$$

where each  $\mathbf{W}$  and each  $\mathbf{U}$  are trainable parameters. The parameters are trained to approximate the formerly defined function  $\mathcal{F}$  for progressive generation.  $\mathbf{h}_t$  is the response of the  $t$ -th stage, forming the predictive results.  $\odot$  denotes element-wise multiplication of tensors and  $\sigma$  is the non-linear activation function, which is  $\tanh$  in practice. After the progressive generation, the convolutional fusion component of the PS-RNN unit learns a robust merging of predicted feature maps. The fusion component helps the prediction for complex textures.

We evaluate the ability for the proposed model to handle complex conditions with a visualization. As shown in Fig. 3, we manually generate several images with regular shapes and immitate the intra prediction context to test the model. We visualize the outputs of the network the proposed PS-RNN. As we can see from the illustration, the network generates satisfactory results for tested contexts.

Though convolutional layers are employed in the framework, these layers are not supposed to directly generate the prediction signals. The size of the kernels in these convolutional layers are small and are designed to extract local features. Thus they are not affected by the asymmetry of the inputs, which disturbs the reconstruction process of CNN based models. The progressiveness of the PS-RNN unit helps mitigate the problem of the asymmetry. The network is capable of handling intra prediction for a wide variety of contexts in a codec.

### C. SATD Loss Function

Though the problems of intra prediction and image inpainting are similar to extent, there are some important differences between them. For image inpainting, especially when a large amount of information is lost, the goal is to construct visually pleasing output images, because the problem is highly ill-posed and it is hard to achieve low pixel-level prediction error. The intra prediction problem, however, is to facilitate the compression of the block. For a transform coding scheme, the goal is to minimize the cost to encode the residue between the original signal and the predicted one.

MSE is the common criterion to train deep networks for many deep learning based image inpainting and intra prediction. For a sample in the training set, the MSE between the prediction value  $\hat{\mathbf{Y}}$  produced by the network and its

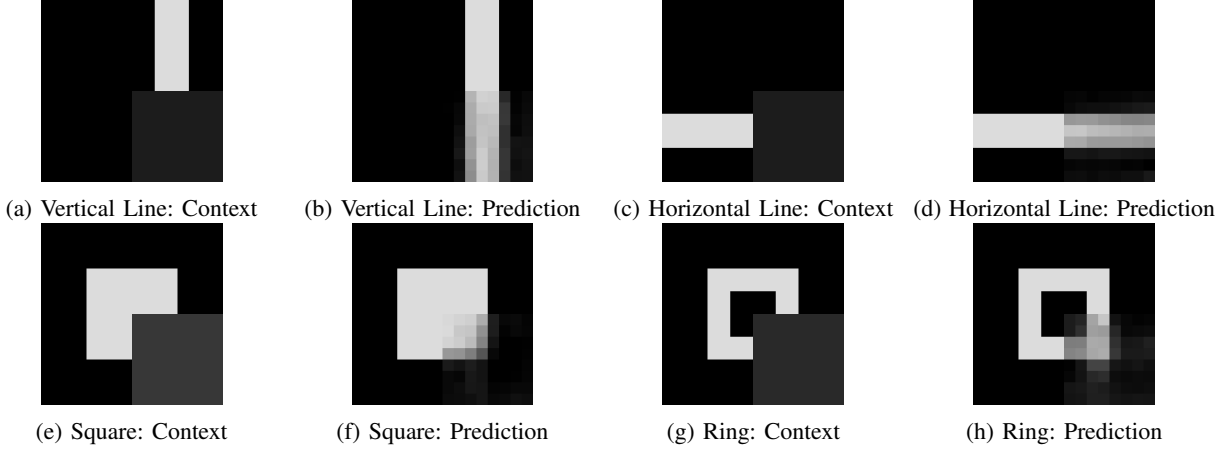


Fig. 3: Visualization of the predictions produced by the proposed model. Combined vertical and horizontal RNN enable the network to handle complex textures.

corresponding ground truth  $\mathbf{Y}$  can be calculated as follows,

$$\text{MSE} = \frac{1}{n} \sum_{j=1}^n \left( \tilde{\mathbf{Y}}_j - \mathbf{Y}_j \right)^2 \quad (3)$$

where  $j$  represents the position of the pixel in the block and  $n$  denotes the total number of pixels in the block.

The MSE loss has drawbacks in training a network for intra prediction. The main goal in intra prediction is to reduce the cost to encode the residue. In the transform coding, the correlation of adjacent predicted pixels matters a lot. However, MSE sums up all the error for each pixel regardless of its position, making it spatially independent. It is not suitable for training a network for video coding. A good loss function for that purpose should be capable of measuring the bit cost caused by spatial correlations.

In our work, we propose to use SATD loss function to train the network for intra prediction tasks. The loss function is inspired by SATD which is used by HEVC as the cost function for RDO and mode decision. Compared with MSE, SATD transforms the residue block using Hadamard transformation before calculating the sum of absolute difference. The transformation is a time-frequency transformation which can concentrate the energy, similar to the one used in transform coding. As a result, the SATD value can better indicate the coding bit-rate cost for this block compared with pixel-wise MSE.

To adopt SATD for network training, we have a closer examination of the calculation of SATD. We define  $\mathbf{D} = \tilde{\mathbf{Y}} - \mathbf{Y}$  as the difference between the prediction  $\tilde{\mathbf{Y}}$  and the ground truth  $\mathbf{Y}$ . Without loss of generality, only the condition where the shape of the Hadamard transform matrix  $\mathbf{H}$  is the same as  $\mathbf{D}$  is illustrated. When  $\mathbf{D}$  is larger in shape, it can be partitioned before the transformation. We apply the transform as,

$$\mathbf{D}' = \mathbf{H}\mathbf{D}\mathbf{H}^T, \quad (4)$$

where  $\mathbf{D}'$  is the transformed difference. Note that the matrix  $\mathbf{H}$  is symmetric,  $\mathbf{D}'$  can also be expressed as,

$$\mathbf{D}' = \mathbf{H}\mathbf{D}\mathbf{H}. \quad (5)$$

We define the SATD loss function  $S$  as,

$$S = \|\mathbf{H}\mathbf{D}\mathbf{H}\|_1 = \sum_i \sum_j |\mathbf{D}'_{ij}|. \quad (6)$$

As the network is trained using the back-propagation method, we calculate the partial derivative of the loss  $S$  with respect to each entry of the distance  $\mathbf{D}$  as,

$$\frac{\partial S}{\partial \mathbf{D}_{kl}} = \frac{\partial \left( \sum_i \sum_j |\mathbf{D}'_{ij}| \right)}{\partial \mathbf{D}_{kl}}. \quad (7)$$

Note that the absolute value function  $y = |x|$  has no valid derivative at the point  $x = 0$ , so we smooth the function by introducing a minor smoothing term  $\epsilon$ . Then the partial derivative turns to,

$$\begin{aligned} \frac{\partial S}{\partial \mathbf{D}_{kl}} &= \frac{\partial \left( \sum_i \sum_j |\mathbf{D}'_{ij}| \right)}{\partial \mathbf{D}_{kl}} \\ &\approx \sum_i \sum_j \frac{\partial \sqrt{\mathbf{D}'_{ij}{}^2 + \epsilon}}{\partial \mathbf{D}_{kl}} \\ &= \sum_i \sum_j \frac{\partial \sqrt{\mathbf{D}'_{ij}{}^2 + \epsilon}}{\partial \mathbf{D}'_{ij}} \cdot \frac{\partial \mathbf{D}'_{ij}}{\partial \mathbf{D}_{kl}} \\ &= \sum_i \sum_j \frac{\mathbf{D}'_{ij}}{\sqrt{\mathbf{D}'_{ij}{}^2 + \epsilon}} \cdot H_{ik} \cdot H_{lj} \\ &= \sum_i \sum_j \frac{\mathbf{D}'_{ij}}{\sqrt{\mathbf{D}'_{ij}{}^2 + \epsilon}} \cdot (H_{ik} \cdot H_{jl}). \end{aligned} \quad (8)$$

The main drawback of MSE in the back-propagation process is that the derivative of  $S$  in MSE loss function with respect to  $\mathbf{D}_{ij}$  is an expression only related to  $\mathbf{D}_{ij}$  itself. As a consequence, the correlations between this pixel and its neighboring pixels are not measured. Differently, SATD measures such correlations to control the bit-rate for encoding the transformed difference  $\mathbf{D}'$ . Thus, the network is trained

towards the goal of optimizing the rate-distortion performance of the codec. We further illustrate this effect in Section IV.

#### D. Variable Block Size

In HEVC, using larger block size saves the bit-rate, as fewer bits are needed to encode block-level flags. Supporting more flexible coding structure is one source of bit-rate reduction of HEVC compared with previous codecs. In directional intra prediction, a large block with simple texture is directly predicted to save bit-rate. However, previous work [16] on employing deep learning in image and video compression restricts the block size for both the anchor and the proposed model to relatively small scale like  $8 \times 8$ . With this restriction, the performance gain of the proposed method in real coding conditions is not fully unveiled.

In our work, variable block size is supported. We allow the size of PU to be from  $4 \times 4$  to  $32 \times 32$ , controlled by the split strategy of HEVC. To train the network for diverse contents scale, we train the network on a diversified dataset where frames of different scale are mixed. In HEVC, all block-sizes share the same intra prediction scheme. When the size of a block is large, its textures tend to be complicated. As a consequence, intra prediction results are more inaccurate for large blocks in HEVC. In our proposed method, we separately train a model for each block-size. One of those is optimized for large blocks. Thus, predictions for large blocks are improved.

#### E. Integration with the HEVC

We implement the network in HEVC Test Model (HM) 16.15. Due to the diversity of the video content, it is hard for a predictor to handle all the conditions. Instead of totally replacing the intra prediction part or overwriting one specific directional mode for the intra prediction of HEVC, we use RDO to decide whether to use the original HEVC predictor or the proposed predictor. For cases where the original predictor can perform well enough, RDO chooses the original HEVC scheme. For other cases where HEVC fails, the network is selected to handle complex texture. One additional flag is added to each PU to indicate the selection. No flag for the directional mode is needed when the proposed model is selected.

Though the reconstructed pixels on the left below of the current PU can be used as reference samples, they are not always available. Fig. 4 shows an example. Only one of four split PUs can have full reference samples as we mentioned above. Other three PUs only have limited reference blocks. To address this issue, the missing pixels for reference are simply filled with DC value in HEVC. In our deep model based intra prediction, filling blocks with constant value brings in extra complexity. Redundant information is fed in the network, which results in poor performance. Thus, we separately train two models for these two conditions. The top-left PU is predicted by a model which is trained using full context. The rest is predicted by a model for the three-block condition where the blocks from above, the left and left-above are used as training context.

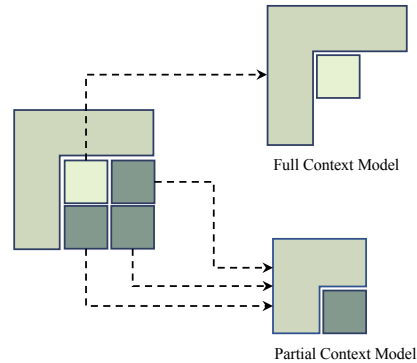


Fig. 4: Different availability of reference samples in a coding unit. Blocks with two different colors are processed using two different models.

## IV. EXPERIMENTAL RESULTS

### A. Training Settings

In data-driven methods, training materials are of great importance. As video frames are quite similar in one sequence, they are not ideal training data for intra prediction models, where content diversity can benefit model training. To effectively train the network, in our proposed method, the training data is generated from high-resolution images provided in [32]. These images include a wide range of contents, including natural view and artificial scenery. They are diversified in texture, color, and brightness which benefits the network training.

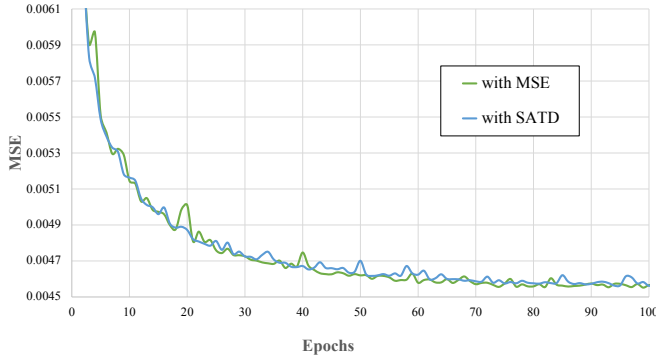
We propose the model to work for various resolutions, so we train the model with materials of various scales. The images are cropped and downsampled to three scales, namely  $1792 \times 1024$ ,  $1344 \times 768$ , and  $896 \times 512$ . Using these images with different scales, our network can work for videos from high resolution to low resolution. Further, to reduce the gap between the distribution of the training set and the test set, the images are previously encoded using HEVC. We set the Quantization Parameter (QP) to 22, 27, 32, 37 and use the reconstructed blocks in the decoding process to form the training pairs. We randomly sample about 3,000,000 pairs to train the model. A training process takes about 4 hours on an NVIDIA GTX 1080 GPU. Adam optimizer [33] is used for training. The network is implemented using TensorFlow [34].

Training the model using pairs with high QP settings can enhance the ability of models to mitigate the influence of the quantization noise, but these training pairs are less expressive. To enhance the robustness to noise while avoiding over-smoothing, the training material is mixed with reconstructed samples in low and high QPs.

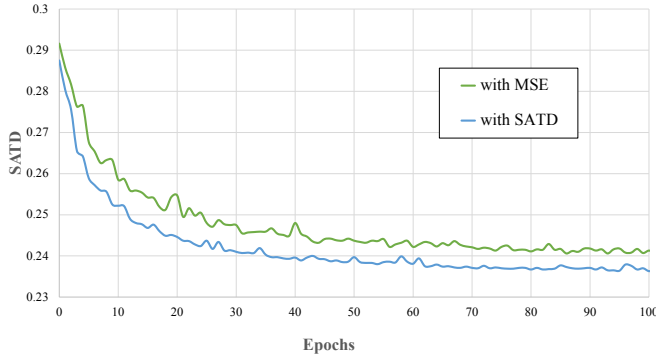
### B. Effectiveness of SATD Loss

We first analyze the SATD loss function. For convenience, we test the performance under the experimental settings where all block-size is restricted to  $8 \times 8$ , for both the anchor and our proposed model. All intra main profile is used in the test. We compare two PS-RNN models trained using MSE loss





(a) Evaluation of MSE



(b) Evaluation of SATD

Fig. 5: Evaluation of MSE and SATD value on the validation set for models trained using MSE and SATD loss function respectively.

function (PS-RNN-MSE) and SATD loss function (PS-RNN-SATD) respectively under the same settings of training data and iterations.

Conventional MSE loss function is not an appropriate objective for training intra prediction network. If the network converges from the view of MSE, it may still fail to converge on Rate-Distortion (RD) cost. As a result, the converged models in close iterations can have a large RD performance gap. Gaps between converged models trained using SATD loss function are much smaller. If the model can converge on SATD loss, it also converges on the RD cost. To make this idea clear, we examine both the MSE value and the SATD value when training the model using MSE and SATD loss function respectively. The result is shown in Fig. 5. Generally, MSE and SATD form a positive correlation. If the model is trained using SATD loss function, the loss on the validation set is significantly lower than that of the model trained using MSE loss function. When evaluated in MSE, we observe that both models converge on similar MSE. However, when interegrated with the codec, the model trained using SATD loss function has superior performance to the model trained using MSE loss function, though they have similar MSE evaluated in the validation set. The quantitative result of this experiment is shown in Table I. It proves that MSE is not an appropriate metrics and objective function for video coding task.

### C. Evaluation of Recurrent Structure

To evaluate the effectiveness of the progressive recurrent structure of the proposed network, we also compare our PS-RNN model with FC networks. To conduct this comparative experiment, we implement an eight-layer FC network (FC-SATD) which has approximately the same amount of parameters as our proposed PS-RNN. Note that in our experiment, to make the comparison fair, both the FC model and PS-RNN model are trained using SATD loss function. The comparison result is shown in BD-Rate [35] in Table I. We also compare the result with the FC network in [16], where the same  $8 \times 8$  block size restriction is applied and MSE is used as the loss function. As we can see from the quantitative result, by introducing the SATD loss function, we achieve a leap in performance for intra prediction using the same FC architecture. We further improve the performance with our proposed PS-RNN network.

### D. Visualization Analysis

To investigate the source of improvement. We visualize the prediction signals of PS-RNN and FC network. We first compare the prediction result of these two network on artificial samples. The contexts and predictions of our proposed PS-RNN model and the FC network are shown in Fig. 6. We also illustrate the prediction results of PS-RNN trained using MSE loss function. From the visualization we can see that, PS-RNN trained using SATD loss function can handle complex texture and the predicted edge is sharp compared with the other two networks. More accurate prediction results contribute to the reduction in overall coding bit-rate.

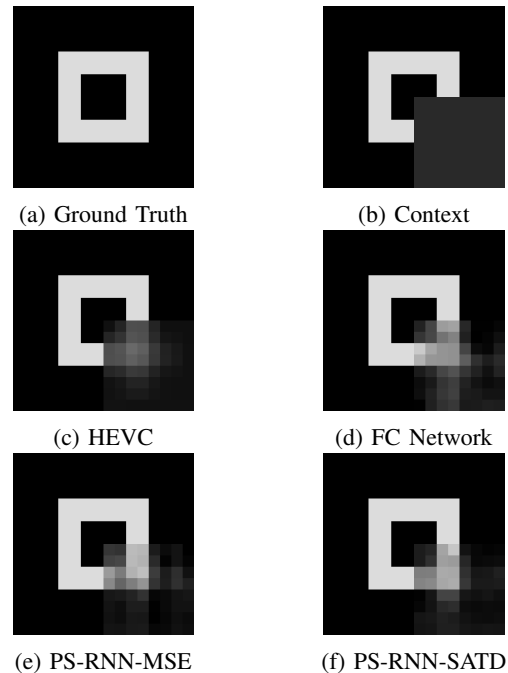


Fig. 6: Prediction results on artificial contexts. We compare the results of three models, namely the FC network trained using SATD loss function, our PS-RNN model trained using MSE and SATD loss function.

TABLE I: Quantitative analysis of selected methods. The result is shown in BD-Rate using HEVC (HM 16.15) as the anchor. PU size is set to  $8 \times 8$  in both the proposed model and the anchor.

Class	Sequence	PS-RNN-SATD	PS-RNN-MSE	FC-SATD	Li [16]
Class A	Traffic	<b>-3.8%</b>	-2.3%	-3.1%	-1.0%
	PeopleOnStreet	<b>-3.8%</b>	-2.2%	-3.1%	-1.3%
	Nebuta(10bit)	<b>-1.9%</b>	<b>-1.9%</b>	<b>-1.9%</b>	-1.6%
	SteamLocomotive(10bit)	<b>-3.2%</b>	-2.8%	<b>-3.2%</b>	-1.7%
	Class A Average	<b>-3.2%</b>	-2.3%	-2.8%	-1.4%
Class B	Kimono	<b>-6.6%</b>	-3.6%	-6.4%	-3.2%
	ParkScene	<b>-3.4%</b>	-1.9%	-2.9%	-1.1%
	Cactus	<b>-3.3%</b>	-1.8%	-2.2%	-0.9%
	BasketballDrive	<b>-7.8%</b>	-3.2%	-3.7%	-0.9%
	BQTerrace	<b>-2.6%</b>	-1.8%	-1.6%	-0.5%
Class B Average	<b>-4.7%</b>	-2.5%	-3.4%	-1.3%	
Class C	BasketballDrill	<b>-2.9%</b>	-1.5%	-1.9%	-0.3%
	BQMall	<b>-2.9%</b>	-1.9%	-1.4%	-0.3%
	PartyScene	<b>-2.3%</b>	-1.8%	-1.1%	-0.4%
	RaceHorses	<b>-2.8%</b>	-2.1%	-2.3%	-0.8%
	Class C Average	<b>-2.7%</b>	-1.8%	-1.7%	-0.5%
Class D	BasketballPass	<b>-2.5%</b>	-1.7%	-1.4%	-0.4%
	BQSquare	<b>-1.8%</b>	-1.2%	-0.8%	-0.2%
	BlowingBubbles	<b>-2.3%</b>	-1.6%	-1.7%	-0.6%
	RaceHorses	<b>-2.6%</b>	-2.5%	-2.2%	-0.6%
	Class D Average	<b>-2.3%</b>	-1.8%	-1.5%	-0.5%
Class E	Johnney	<b>-6.8%</b>	-3.8%	-4.7%	-1.0%
	FourPeople	<b>-5.6%</b>	-2.8%	-4.1%	-0.8%
	KristenAndSara	<b>-6.6%</b>	-2.9%	-4.0%	-0.8%
	Class E Average	<b>-6.3%</b>	-3.2%	-4.3%	-0.9%
Average		<b>-3.8%</b>	-2.3%	-2.7%	-0.9%

We also evaluate the predictions in natural cases. We compare PS-RNN with FC model in this experiment. The result is shown in Fig. 7. We can see that in real coding conditions, our model achieves better accuracy in prediction with lower MSE. Since the FC network does not investigate the correlations between adjacent pixels, the prediction signals lack the structural accuracy. The progressiveness of PS-RNN keeps the structure of the edges in the original image.

#### E. Variable Block Size Analysis

In real conditions, variable-block-size coding is used to further save bit-rate. If the predictions for large blocks are accurate, there is no need to split the blocks and do separate prediction for each of the smaller blocks. For HEVC, simply allowing a two-level split in block size brings 7% bit-rate reduction. To evaluate our proposed model in real coding conditions, we remove the restriction on block size. The testing experiment is conducted on Common Test Conditions [36]. In our experiments, we set the scale of Coding Units (CU) to be up to  $32 \times 32$ , allowing split for intra prediction. The size of PU ranges from  $4 \times 4$  to  $32 \times 32$  and is adaptively decided by RDO. We train a different model for each coding block size, respectively. As we evaluate the method in all intra configuration, only the first frame of each sequence is tested.

The result is illustrated in gain in BD-Rate shown in Table II. The quantitative results show the improvement in rate-distortion performance using our proposed intra prediction method.

We illustrate the results of RDO selection in Fig. 8. On average about 35% PUs are predicted using PS-RNN in all-intra mode, which reflects the gain in performance.

#### V. CONCLUSION

In this paper we propose PS-RNN to improve intra prediction performance in video coding. The model is end-to-end trained to handle complex textures, making it capable of predicting for various content. The progressive generation of predictions addresses the problem of asymmetry in intra prediction. To further enhance the usability of the network in the codec, we propose to use SATD loss function for network training. It calculates both the distortion and the corresponding bit-rate for encoding the residue. Our network supports variable block size in HEVC, bringing a leap in real coding performance. The proposed method achieves on average 2.4% bit-rate reduction under the same reconstruction quality compared with HEVC.



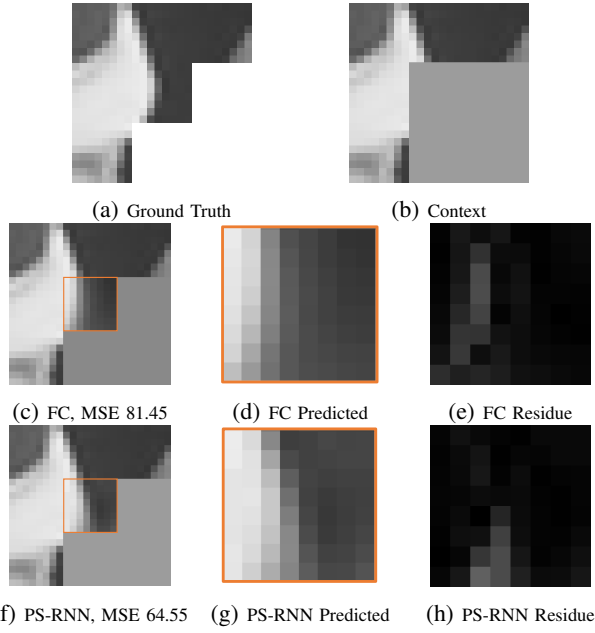


Fig. 7: Prediction results on natural context. We compare the results of two models, the FC network and our PS-RNN model. We also show the residual map and the MSE of the prediction signals to show that PS-RNN provides more accurate prediction results.



(a) For this frame, about 47% of blocks are predicted using PS-RNN.



(b) We crop a region of size  $416 \times 240$  in the original frame. For this frame, about 50% of blocks are predicted using PS-RNN.

Fig. 8: Results of RDO selection of a frame in the sequence (a) *RaceHorses* and (b) *FourPeople*. Blocks with green borders are predicted by PS-RNN.

TABLE II: Performance evaluated in BD-Rate using all-intra main configurations. The anchor is HM 16.15. The first frame of each sequence is tested.

Class	Sequence	BD-Rate		
		Y	U	V
Class A	Traffic	-3.27%	-2.63%	-2.40%
	PeopleOnStreet	-3.96%	-2.49%	-2.10%
	NebutaFestival	-0.62%	-0.74%	-0.66%
	SteamLocomotiveTrain	-0.83%	-1.11%	-2.70%
	Class A Average	-2.17%	-1.74%	-1.97%
Class B	Kimono	-1.23%	-0.87%	-0.94%
	ParkScene	-2.67%	-1.58%	-1.32%
	Cactus	-2.34%	-1.50%	-0.88%
	BasketballDrive	-1.40%	-1.15%	-1.44%
	Class B Average	-2.01%	-1.13%	-1.02%
Class C	BasketballDrill	-1.56%	-0.35%	-1.50%
	BQMall	-3.00%	-1.41%	-0.02%
	PartyScene	-2.48%	-2.16%	-2.21%
	RaceHorses	-2.28%	-1.85%	-0.97%
Class C Average	-2.33%	-1.44%	-1.17%	
Class D	BasketballPass	-2.08%	-1.89%	-0.52%
	BQSquare	-2.06%	-0.58%	1.81%
	BlowingBubbles	-2.70%	-2.16%	0.48%
	RaceHorses	-3.52%	-3.26%	-1.83%
Class D Average	-2.59%	-1.97%	-0.01%	
Class E	Johnney	-3.56%	-1.33%	-2.43%
	FourPeople	-3.75%	-3.58%	-3.89%
	KristenAndSara	-3.09%	-3.52%	-1.17%
	Class E Average	-3.47%	-2.81%	-2.49%
Average	-2.44%	-1.74%	-1.26%	

## REFERENCES

- [1] T. Wiegand, G. J. Sullivan, G. Bjontegaard, and A. Luthra, "Overview of the H.264/AVC video coding standard," *IEEE Transactions on Circuits and Systems for Video Technology*, vol. 13, no. 7, pp. 560–576, 2003.
- [2] J. Lainema, F. Bossen, W.-J. Han, J. Min, and K. Ugur, "Intra coding of the HEVC standard," *IEEE Transactions on Circuits and Systems for Video Technology*, vol. 22, no. 12, pp. 1792–1801, 2012.
- [3] G. J. Sullivan and T. Wiegand, "Rate-distortion optimization for video compression," *IEEE Signal Processing Magazine*, vol. 15, no. 6, pp. 74–90, 1998.
- [4] J. Li, B. Li, J. Xu, and R. Xiong, "Efficient multiple line-based intra prediction for HEVC," *IEEE Transactions on Circuits and Systems for Video Technology*, vol. 28, no. 4, pp. 947–957, 2016.
- [5] —, "Intra prediction using multiple reference lines for video coding," in *Proc. of Data Compression Conference*, 2017.

- [6] R. Wei, R. Xie, L. Song, L. Zhang, and W. Zhang, "Improved intra angular prediction with novel interpolation filter and boundary filter," in *Proc. of Picture Coding Symposium*, 2016.
- [7] C.-H. Yeh, T.-Y. Tseng, C.-W. Lee, and C.-Y. Lin, "Predictive texture synthesis-based intra coding scheme for advanced video coding," *IEEE Transactions on Multimedia*, vol. 17, no. 9, pp. 1508–1514, 2015.
- [8] H. Chen, T. Zhang, M.-T. Sun, A. Saxena, and M. Budagavi, "Improving intra prediction in high-efficiency video coding," *IEEE Transactions on Image Processing*, vol. 25, no. 8, pp. 3671–3682, 2016.
- [9] T. Zhang, H. Chen, M.-T. Sun, D. Zhao, and W. Gao, "Hybrid angular intra/template matching prediction for HEVC intra coding," in *Proc. of Visual Communications and Image Processing*, 2015.
- [10] X. Qi, T. Zhang, F. Ye, A. Men, and B. Yang, "Intra prediction with enhanced inpainting method and vector predictor for HEVC," in *Proc. of IEEE International Conference on Acoustics, Speech and Signal Processing*, 2012.
- [11] D. Liu, X. Sun, F. Wu, S. Li, and Y.-Q. Zhang, "Image compression with edge-based inpainting," *IEEE Transactions on Circuits and Systems for Video Technology*, vol. 17, no. 10, pp. 1273–1287, 2007.
- [12] N. P. Jouppi, C. Young, N. Patil, D. Patterson, G. Agrawal, R. Bajwa, S. Bates, S. Bhatia, N. Boden, A. Borchers *et al.*, "In-datacenter performance analysis of a tensor processing unit," in *Proc. of Annual International Symposium on Computer Architecture*, 2017.
- [13] S. Xia, W. Yang, Y. Hu, S. Ma, and J. Liu, "A group variational transformation neural network for fractional interpolation of video coding," in *Proc. of Data Compression Conference*, 2018.
- [14] X. Zhang, W. Yang, Y. Hu, and J. Liu, "DMCNN: Dual-domain multi-scale convolutional neural network for compression artifacts removal," in *Proc. of IEEE International Conference on Image Processing*, 2018.
- [15] Z. Liu, X. Yu, S. Chen, and D. Wang, "CNN oriented fast HEVC intra CU mode decision," in *IEEE International Symposium on Circuits and Systems*, 2016.
- [16] J. Li, B. Li, J. Xu, and R. Xiong, "Intra prediction using fully connected network for video coding," in *Proc of IEEE International Conference on Image Processing*, 2017.
- [17] W. Cui, T. Zhang, S. Zhang, F. Jiang, W. Zuo, Z. Wan, and D. Zhao, "Convolutional neural networks based intra prediction for HEVC," in *Proc. of Data Compression Conference*, 2017.
- [18] G. J. Sullivan, J. Ohm, W.-J. Han, and T. Wiegand, "Overview of the high efficiency video coding (HEVC) standard," *IEEE Transactions on Circuits and Systems for Video Technology*, vol. 22, no. 12, pp. 1649–1668, 2012.
- [19] T. Nguyen and D. Marpe, "Objective performance evaluation of the HEVC main still picture profile," *IEEE Transactions on Circuits and Systems for Video Technology*, vol. 25, no. 5, pp. 790–797, 2015.
- [20] L. Theis, W. Shi, A. Cunningham, and F. Huszár, "Lossy image compression with compressive autoencoders," in *Proc. of International Conference on Learning Representations*, 2017.
- [21] J. Ballé, V. Laparra, and E. P. Simoncelli, "End-to-end optimized image compression," in *Proc. of International Conference on Learning Representations*, 2017.
- [22] K. Gregor, F. Besse, D. J. Rezende, I. Danihelka, and D. Wierstra, "Towards conceptual compression," in *Proc. of Advances In Neural Information Processing Systems*, 2016.
- [23] E. Agustsson, F. Mentzer, M. Tschannen, L. Cavigelli, R. Timofte, L. Benini, and L. V. Gool, "Soft-to-hard vector quantization for end-to-end learning compressible representations," in *Proc. of Advances in Neural Information Processing Systems*, 2017.
- [24] G. Toderici, D. Vincent, N. Johnston, S. Jin Hwang, D. Minnen, J. Shor, and M. Covell, "Full resolution image compression with recurrent neural networks," in *Proc. of IEEE International Conference on Computer Vision and Pattern Recognition*, 2017.
- [25] M. H. Baig, V. Koltun, and L. Torresani, "Learning to inpaint for image compression," in *Proc. of Advances in Neural Information Processing Systems*, 2017.
- [26] C. Ballester, M. Bertalmio, V. Caselles, G. Sapiro, and J. Verdera, "Filling-in by joint interpolation of vector fields and gray levels," *IEEE Transactions on Image Processing*, vol. 10, no. 8, pp. 1200–1211, 2001.
- [27] M. Bertalmio, G. Sapiro, V. Caselles, and C. Ballester, "Image inpainting," in *Proc. of Annual Conference on Computer Graphics and Interactive Techniques*, 2000.
- [28] V. Kwatra, I. Essa, A. Bobick, and N. Kwatra, "Texture optimization for example-based synthesis," in *ACM Transactions on Graphics*, 2005.
- [29] J. Liu, S. Yang, Y. Fang, and Z. Guo, "Structure-guided image inpainting using homography transformation," *IEEE Transactions on Multimedia*, 2018.
- [30] C. Yang, X. Lu, Z. Lin, E. Shechtman, O. Wang, and H. Li, "High-resolution image inpainting using multi-scale neural patch synthesis," in *Proc. of IEEE Conference on Computer Vision and Pattern Recognition*, 2017.
- [31] D. Pathak, P. Krahenbuhl, J. Donahue, T. Darrell, and A. A. Efros, "Context encoders: Feature learning by inpainting," in *Proc. of IEEE Conference on Computer Vision and Pattern Recognition*, 2016.
- [32] R. Timofte, E. Agustsson, L. Van Gool, M.-H. Yang, L. Zhang *et al.*, "NTIRE 2017 challenge on single image super-resolution: Methods and results," in *Proc. of IEEE Conference on Computer Vision and Pattern Recognition Workshop*, 2017.
- [33] D. Kingma and J. Ba, "Adam: A method for stochastic optimization," *Proc. of International Conference for Learning Representations*, 2015.
- [34] M. Abadi, A. Agarwal, P. Barham, E. Brevdo, Z. Chen, C. Citro, G. S. Corrado, A. Davis, J. Dean, M. Devin, S. Ghemawat, I. Goodfellow, A. Harp, G. Irving, M. Isard, Y. Jia, R. Jozefowicz, L. Kaiser, M. Kudlur, J. Levenberg, D. Mané, R. Monga, S. Moore, D. Murray,

- C. Olah, M. Schuster, J. Shlens, B. Steiner, I. Sutskever, K. Talwar, P. Tucker, V. Vanhoucke, V. Vasudevan, F. Viégas, O. Vinyals, P. Warden, M. Wattenberg, M. Wicke, Y. Yu, and X. Zheng, “TensorFlow: Large-scale machine learning on heterogeneous systems,” 2015, software available from tensorflow.org. [Online]. Available: <https://www.tensorflow.org/>
- [35] G. Bjontegarrd, “Calculation of average psnr differences between rd-curves,” *VCEG-M33*, 2001.
- [36] F. Bossen, “Common test conditions and software reference configurations,” in *Joint Collaborative Team on Video Coding (JCT-VC) of ITU-T SG16 WP3 and ISO/IEC JTC1/SC29/WG11, 5th meeting, Jan. 2011*, 2011.